Renewable Energy 77 (2015) 9–14

Contents lists available at ScienceDirect

Renewable Energy

journal homepage: www.elsevier.com/locate/renene

Experimental results on power absorption from a wave energy converter at the Lysekil wave energy research site

Erik Lejerskog*, Cecilia Boström, Ling Hai, Rafael Waters, Mats Leijon

Swedish Centre for Renewable Electric Energy Conversion, Division for Electricity Research, Department of Engineering Science, Uppsala University, Box 534, 75121 Uppsala, Sweden

ARTICLE INFO

Article history:
Received 20 December 2013
Accepted 17 November 2014
Available online 18 December 2014

Keywords:
Wave energy conversion
Offshore experiments
Linear generator
Power take-off
System optimization
Power absorption

ABSTRACT

Power generation from wave power has a large potential to contribute to our electric energy production, and today, many wave power projects are close to be commercialized. However, one key issue to solve for many projects is to decrease the cost per installed kW. One way to do this is to investigate which parameters that have a significant impact on the wave energy converters (WEC) performance.

In this paper, experimental results on power absorption from a directly driven point absorbing WEC are presented. The experiments have been carried out at the Lysekil research site in Sweden. To investigate the performance of the WEC, the absorbed power and the speed of the translator are compared. The result confirms that the buoy size and the translator weight have a large impact on the power absorption from the generator. By optimizing the buoy size and translator weight, the WEC is believed to produce power more evenly over the upward and downward cycle.

Moreover, to predict the maximum power limit during normal operation, a simulation model has been derived. The results correlates well with experimental data during normal operation.

1. Introduction

The energy demand is continuously increasing worldwide and conventional methods for power generation are causing many environmental issues such as global warming, acid rain and air pollution. Harnessing natural resources and converting them into electric power can be an effective solution to ease the conflicts between large energy demand and environment pollution. Among all sources of renewable energy, wave energy has the highest energy density [1], and is considered as a promising alternative energy resource for the future. In 2012, the worldwide installed ocean power capacity was approximately 6 MW and in the next coming years this number is believed to increase to 35 MW [2]. The research within this area has come far and two review articles of different types of WEC technologies and their progress are given in Refs. [2,3].

Uppsala University has developed a wave energy converter (WEC) that uses a point absorber directly driving a linear generator for power production, see Fig. 1a. Various efforts have been made to optimize the system in order to decrease the cost per installed kW and to increase the reliability. In general the use of directly driven generators, or generators moving with a variable speed, have increased in renewable energy applications, particularly in the wind industry. Most of the developers have switched from using a fixed speed technology to a variable speed technology [4]. The main reason for the change is the increased power absorption (power capture ratio) which can be achieved with a variable speed control. The rotation speed can be controlled with power electronics according to wind speed to maximise the power production. A direct drive approach also has other benefits such as less maintenance work since mechanical parts that are otherwise needed between a conventional generator and the low speed motion of the waves, like turbines, gear boxes etc., are not needed. However, a direct drive approach tends to have a somewhat more complicated electrical system since a conversion system is required before the connection to the grid. Furthermore, a generator moving with low speed is larger compared to a 50 Hz generator with the same power rating. In the wave power area there exists a number of different projects developing linear and directly driven generators, some examples are given in Refs. [5–10].

* Corresponding author. Tel.: +46 18 471 5870.
E-mail address: erik.lejerskog@angstrom.uu.se (E. Lejerskog).

http://dx.doi.org/10.1016/j.renene.2014.11.050

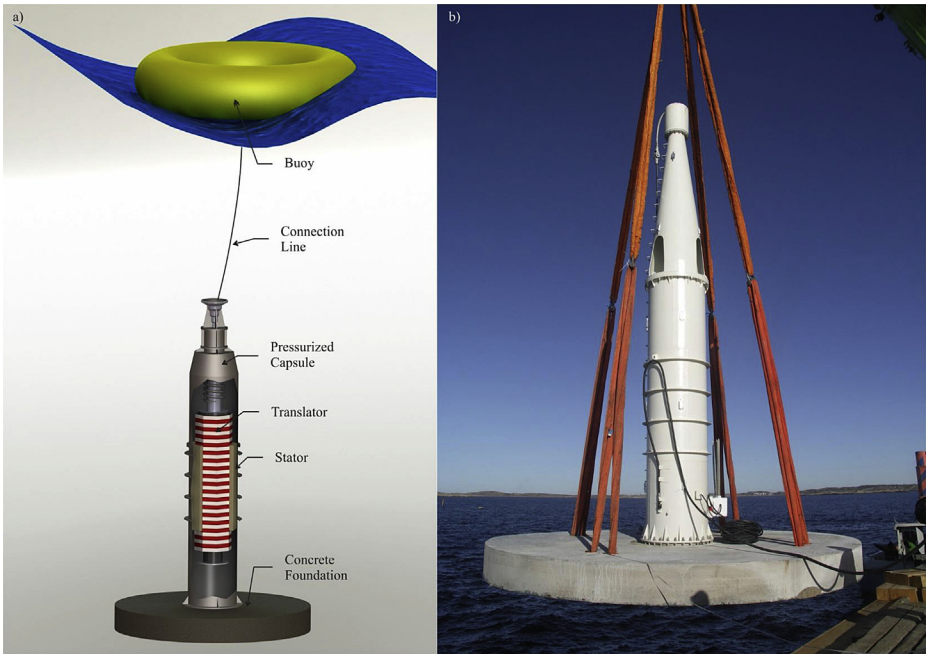

Fig. 1. a) Illustration of the WEC developed at Uppsala University. b) Picture of L9 during deployment.

In 2006, Uppsala University deployed their first WEC, the L1 [11]. Since then more than 10 WECs have been deployed at the research site located on the Swedish west coast, outside the town Lysekil. The research site is equipped with a 3 km long subsea cable that connects the WECs to a measuring station on a close by island, Hermanö. In the measuring station, voltage and current data from the WECs are stored. More information about the research site is given in Refs. [12,13].

The WEC consists of a buoy at the surface, which is connected through a connection line (steel wire) to a linear generator placed in a capsule on the seabed, Fig. 1a. To keep the WEC on the seabed, a concrete foundation with a weight of 35 tonnes is attached at the bottom of the capsule. When the buoy moves with the motion of the waves, the translator inside the linear generator will follow the motion in heave, thus inducing a varying magnetic flux in the stationary stator windings.

The power output from the WEC is influenced by a number of different parameters like the buoy size, translator weight, damping etc. To be able to increase the generated power from the WEC it is important to know how it behaves during a full cycle i.e. both when the buoy and translator moves upwards and downwards, the purpose with this work is to study this further. In this paper, the power absorption of a second generation WEC known as the L9 is studied both experimentally and analytically. The L9 was deployed at the Lysekil research site in 2009. A picture taken during deployment is presented in Fig. 1b.

To predict the impact of buoy volume and translator weight, a static model has been derived to find the power limits at different speeds during the upward and downward cycle. The results from the simulations could be used as a design tool early in the design process of a WEC. To verify the model, it has been compared with experimental results for different load conditions.

1.1. Experiments

The experiments were carried out at the offshore research site on the Swedish west coast. Details about the WEC, L9, used in the offshore experiments and details about the measurements done are presented in this section.

1.2. Linear generator

The generator is a linear generator shaped as an octagon, i.e. it has eight sides, see Fig. 2. The stator-sides are made up of thin electric steel sheets and are wound with a three phase winding. The stator-sides are then attached to the capsule walls. The translator has eight sides of surface mounted Ne-Fe-B magnets. To keep a low friction for the motion of the translator and to maintain a 3 mm air-gap between the stator-sides and the magnets, four rails mounted on the translator and 84 wheels divided into four rails are mounted on the capsule. The stator-sides and the translator have the same vertical length. This equal length makes the active area of the generator to change when the translator deviates from its center position. To keep the generator sealed from seawater a piston rod is attached to the translator. When the translator moves up and down, the piston rod will move through a seal housing placed on the top of the capsule. Some of the main parameters of the generator are presented in Table 1.

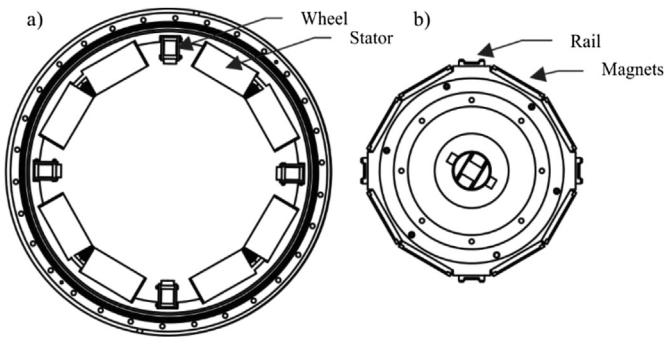

Fig. 2. a) Design of the stator inside the capsule. b) The translator with mounted permanent magnets.

Table 1
Parameters of the generator L9.

Quantity	Value
Voltage[a]	450 V
Nominal power	20 kW
Pole width (ω_p)	55.8 mm
Translator length	2000 mm
Stator length	1961.5 mm
Translator weight (m_t)	2700 kg
Stroke length	1976.5 mm

[a] Line to line voltage when the speed of the translator is 0.7 m/s.

1.3. Point absorbing buoy

The experiments were carried out with a torus shaped buoy, assembled together from six sections, see Fig 3. It was equipped with a line force measurement system, consisting of a force transducer, battery, data logging and transmission system and an antenna. A tripod connects the buoy to the connection line which, in turn, connects to the generator. The volume of the buoy was 13.4 m^3 and it had a total weight of 3500 kg.

1.4. Measurments

The measurements were carried out in a measurement station located 2 km south-east of the research site. A three phase subsea power cable connects the WEC to the station. During the experiments the measuring station was equipped with three different delta connected resistive loads, 4.9 Ω, 11 Ω and 20 Ω. The values of the resistance in the three cases are presented as one of the three resistors in the delta connection. Current and voltage out from the WEC are measured in the station with a sampling frequency of 256 Hz. The data is stored locally and accessible through a remote communication system.

The power dissipated in the load is calculated from the measured voltages (V_a, V_b, V_c) and currents (I_a, I_b, I_c) as:

$$P_{\text{load}} = V_a I_a + V_b I_b + V_c I_c \tag{1}$$

The output power, P_{out}, from the WEC is calculated by adding the power loss, P_{loss}, from the cables as:

Fig. 3. Torus buoy used in the experiment.

$$P_{\text{loss}} = R\left(I_a^2 + I_b^2 + I_c^2\right) \tag{2}$$

$$P_{\text{out}} = P_{\text{load}} + P_{\text{loss}} \tag{3}$$

The speed of the translator is calculated by finding the zero crossings of the voltage out from the WEC and by knowing the pole width in the generator, ω_p. The speed is calculated as:

$$v = \frac{\omega_p}{\Delta t} \tag{4}$$

1.5. Error analysis

When the translator is situated at the top or bottom position, noise is induced in the voltage measuring signal close to the zero crossings. The noise is visible as peaks in the speed due to small Δt of the noise at almost zero power. A filter was used to reduce these peaks, but some of the noise is still visible in the results.

Other parameters that influence the accuracy of the measurements are: the accuracy of the resistance in the generator windings (1 ± 1.5% Ω per phase), the accuracy of the subsea cable resistance (0.54 ± 1.5% Ω per phase) and the accuracy of the resistive loads at the station. Also the voltage measurement system has an estimated accuracy of ±1.5% and the current measurement has an estimated accuracy of ±0.5%.

1.6. Simulation model

To predict the behavior of the WEC a static model has been derived where the limits in power out from the WEC is based on the volume of the buoy and the mass of the translator. To find the limits the forces in the system can be written as:

$$F_b \geq F_{\text{em}} + \text{mg} \tag{5}$$

where F_b is the buoyancy force, F_{em} is the electromagnetic force and m is the mass of the system. By using the relation between absorbed power, electromagnetic force and the speed:

$$P_{\text{abs}} = F_{\text{em}} v \tag{6}$$

The limit of maximum power absorption when the translator moves upwards can be calculated as:

$$P_{\text{abs}} = (F_{\text{bTot}} - (m_b + m_t)g)v \tag{7}$$

where F_{bTot} is the buoyancy force of a completely submerged buoy, m_b and m_t are the buoy weight and the translator weight.

When the translator is moving downwards, the limit of the absorbed power is calculated as:

$$P_{\text{abs}} = m_t g v \tag{8}$$

assuming that the gravitational force of the translator is equal to the damping force of the generator.

2. Results

The power from the WEC is plotted on the y-axis against the translator speed on the x-axis during different load cases and varying wave climates is shown in Figs. 4–6. The blue (in web version) dots represent the power when the translator moves upwards and the red (in web version) dots represent the power when the translator moves downwards. The upper dash-dotted black lines are the simulated maximum value of the power when the

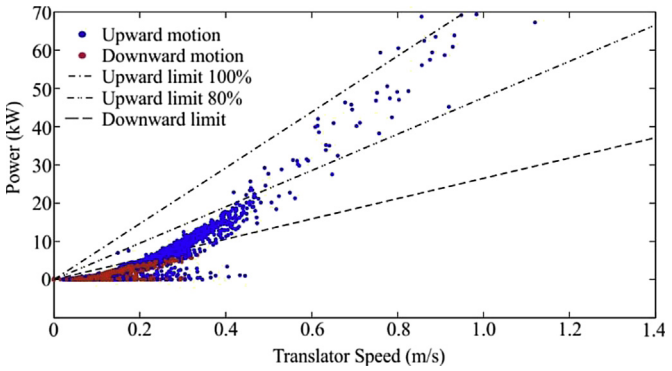

Fig. 4. Simulated and experimental results of the WEC when it is connected to 4.9 Ω loads.

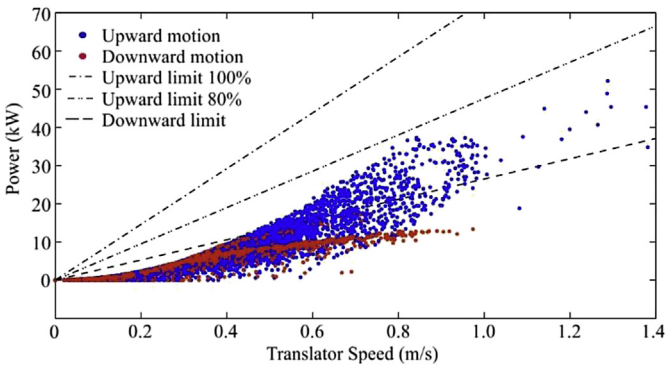

Fig. 6. Simulated and experimental results of the WEC when it is connected to 20 Ω loads.

translator moves upwards. 100% stands for a completely submerged buoy and 80% for a buoy submerged to 80%. The lower dash-dotted black line represents the simulated maximum value of the power when the translator moves downwards.

In Fig. 4, the WEC is connected to a 4.9 Ohm load. The significant wave height during the experiment was around 3 m. It's noticeable that a number of upward motion data points exceed the 100% upward limit. But most of the data points are below the 80% limit. However, in the downward motion, no data points are reaching the downward simulated limit.

In Fig. 5, the WEC is connected to an 11 Ohm load. The significant wave height during this period was around 1.5 m. During this load case, there are only a few observations, blue (in web version) dots, reaching above the 80% upward limit and non above the 100% limit. In the downward direction two trends of the observations, red (in web version) dots, are slightly visible.

In Fig. 6, the WEC is connected to a 20 Ohm load and the significant wave height was around 2 m. In this result, the two trends in the downward motion, red (in web version) dots, are more visible compared to the results in Fig. 5. Moreover, during the upward motion no observations are reaching the 80% upward limit. The observations, blue (in web version) dots, in Fig. 6 are more spread out, especially at higher speeds if compared with Figs. 4 and 5.

The results in Figs. 7–9 present the three phase voltage during 1 min from the different load cases studied in Figs. 4–6. The voltages presented are all included in the results of Figs. 4–6. The voltages in Fig. 7 and 8 were chosen to further analyze the high peaks in power during the upward motion that were visible in the results in Figs. 5 and 6. The voltage in Fig. 9 represents a sequence when the power production form the WEC was high, and will be represented as data points with high speed in Fig. 6.

In Fig. 7, for the 4.9 Ω load, high peaks in the voltage are occurring frequently and seems to be found at turning points of the translator. Also a reduction in the voltage is visible when the translator is on its way down, this is highlighted in the figure.

Fig. 8, presents the voltage when the WEC is connected to an 11 Ω load. As in Fig. 7, high peaks in the voltage are visible but they are not as frequent.

In Fig. 9, the voltage is presented when the WEC is connected to a 20 Ω load. No high peaks in the voltage are visible during this period. When the translator is moving downwards an increase in the voltage is visible in the beginning, then the voltage drops fast and then starts to increase again until the translator reach the bottom turning point.

3. Discussion

From the results in Figs. 4–6 the trend is clear, the absorbed power is higher when the translator moves upwards, a result which is also predicted by the model. By increasing the weight of the translator the downward power could be increased, however at a cost of a decrease in the power upwards. By fine-tuning the buoy volume, weight and the translator weight an optimum could be reached. Other parameters such as wave climate and generator design need to be decided before this fine-tuning can begin. A general thought could be to increase the buoy volume and the translator weight to increase the power absorbed. But a too large buoy and translator weight will not give good results in a wave climate with little energy and vice versa, and also other limitations

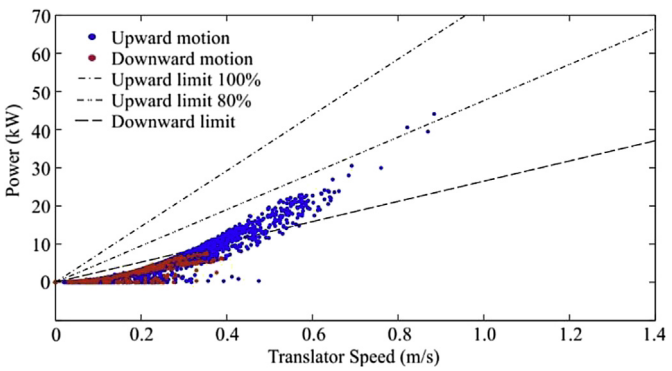

Fig. 5. Simulated and experimental results of the WEC when it is connected to 11 Ω loads.

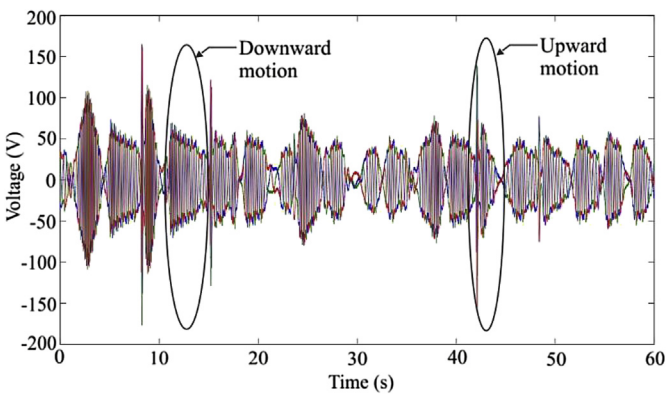

Fig. 7. Measured three phase voltage at 4.9 Ω load.

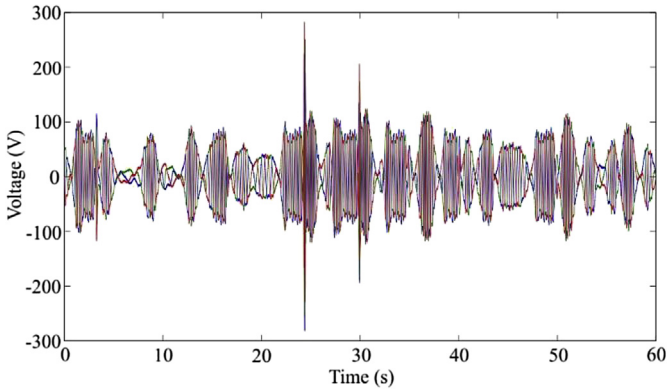

Fig. 8. Measured three phase voltage at 11 Ω load.

would arise at high power levels and speeds such as current and voltage limitations in the windings.

When the translator moves downwards, the results in Figs. 5–6 show two trend lines. This could be due to the changing active area of the stator. When the translator has moved to the top point the active stator area has a minimum, resulting in lower damping, which will allow the translator to move faster when it moves downwards and thus resulting in higher voltage. This is connected to the higher trend line. When the translator has moved to the midpoint, the active area and damping has a maximum and the translator moves slower, with a lower voltage. This is the starting point on the lower trend line. When the translator moves down towards the bottom point the active area decreases with an increase in voltage and lower damping. This is indicated by the increasing power and speed on the lower trend line. This can also be seen in the three phase voltage in Figs. 8 and 9. During the downwards motion of the translator, the speed is higher when the active area is small and vice versa.

In the simulation model used in this paper dynamic forces from ocean waves such as excitation force and radiation force were neglected, but the experimental results show that for most cases, at the studied site, it is enough to consider only the buoyancy force to estimate upper limit of power production. By using a rough model based on fundamental physics the time spent on simulations can be reduced. Moreover, it can help to find parts in the system where a more comprehensive study is needed to model the system, thus making the heavy calculations where they are needed instead of performing a complete dynamic simulation of the entire system. For a real time power production model, it would be necessary to include dynamic forces [14,15].

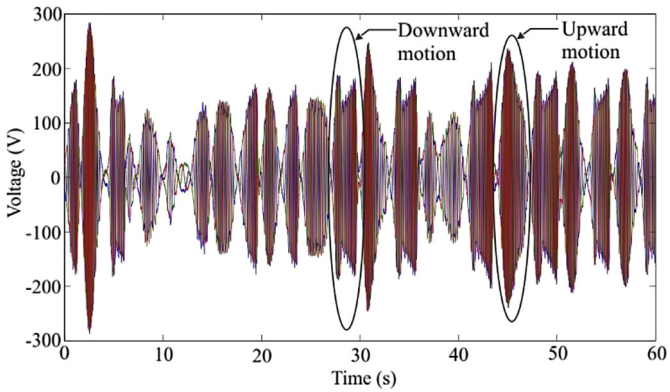

Fig. 9. Measured three phase voltage at 20 Ω load.

The model doesn't consider different buoy shape, e.g. cylinder or torus, which would affect the system performance mainly by different in added mass. Only volume and mass of the buoy have been considered, through again, experimental results indicate that the model works well enough. It would be very interesting to compare the power production from two differently shaped buoys with the same weight and volume, which is a topic for future work together with an improved model with information of buoy shape.

The motive behind using an 80% limit in the upward direction is that the peaks in power are generally below this limit. This limit indicates the power limitation during normal operation and data points exceeding this limit are mainly due to non-desirable effects. In Fig. 4 there are some peaks reaching over the 100% upward limit and a large number reaching over the 80% limit. By studying the voltage when these peaks arise in Figs. 7–8, it is quite clear where these peaks come from. The peaks occur when the translator is positioned in its lowest position and is starting to move upwards. Furthermore, the decreasing voltage amplitude before these peaks are also quite similar. As the translator moves downwards the damping gets higher and higher, almost bringing the translator to a stop. Because of this, the buoy and the connection line move downwards with a higher speed than the translator resulting in the connection line becoming slack. When a new wave lifts the buoy again, a snatch load occurs resulting in a short period of high speed and high voltage and current. It seems to happen more frequent when the generator has a higher damping, most frequent at 4.9 Ω but also visible at 11 Ω and 20 Ω load cases. The higher occurrence of the power peaks in Fig. 4, could partly arise due to a more powerful wave climate at this time, with a significant wave height of about 3 m. These snatch loads were also detected in the first generation of WECs, [16]. With a higher weight of the translator this could be avoided, or the snatch loads would instead occur at another load with even higher damping. Snatch loads are not included in the simulation model and are not a desirable effect, but it explains why there are peaks going higher than the simulated limit for the upward motion.

4. Conclusion

The experimental results prove, as expected from the simulation model, that higher power is produced when the translator moves upwards compared to when it moves downwards. This is mainly due to that the lifting force of the buoy greatly exceeds the downward force of the translator. By increasing the weight of the translator a more evenly distributed and higher average power output could be achieved.

When the translator moves downwards, the power has two visible trends in load the cases 11 Ω and 20 Ω, due to the changing active area in the generator.

The experiments shows that by having the same vertical length of the stator-sides and the translator, the speed near the endpoints increases at the expense of active stator area between the stator and the magnets. It also shows that the speed has a greater influence on the voltage compared to the active stator area.

When the damping of the generator goes up, i.e. when the resistance of the load goes down, the peaks in the power, induced by the snatch-loads, occur more frequently. This is seen in Figs. 4 and 5, with a resistive load of 4.9 Ω and 11 Ω respectively. These peaks occur when the translator has reached its lower turning point and is starting to move upwards.

The simulation model has been verified and works during normal conditions. The simulated downward limit is not reached in any of the experiments, and in the 11 Ω and 20 Ω load case, the 100% upward limit is not reached.

Acknowledgments

The authors would like to thank, Swedish Research Council under Grant no. 2009-3417, Statkraft AS, Fortum OY, the Swedish Energy Agency, Seabased Industry AB, Draka Cable AB, the Gothenburg Energy Research Foundation, Falkenberg Energy AB, Helukabel, Proenviro, ÅF Group, Vinnova, the Foundation for the Memory of J. Gust Richert, the Göran Gustavsson Research Foundation, Vargöns Research Foundation, Swedish Research Council grant no. 621-2009-3417 and the Wallenius Foundation for their support of the project.

References

[1] Clément A, McCullen P, Falcão A, Fiorentino A, Gardner F, Hammarlund K, et al. Wave energy in Europe: current status and perspectives. Renew Sustain Energy Rev 2002;6(5):405–31.
[2] IEA-OES. International energy agency implementing agreement on ocean energy systems. OES-IA, Annual Report 2012. IEA-OES Executive Committee; 2012.
[3] Falcão AFO. Wave energy utilization: a review of the technologies. Renew Sustain Energy Rev 2010;4(3):899–918.
[4] Li H, Chen Z. Overview of different wind generator systems and their comparisons. IET Renew Power Gener 2008;2(2):123–38.
[5] Rhinefrank K, Agamloh EB, von Jouanne A, Wallace AK, Prudell J, Kimble K, et al. Novel ocean energy permanent magnet linear generator buoy. Renew Energy 2006;31(9):1279–98.
[6] Crozier R, Bailey H, Mueller M, Spooner E, McKeever P. Analysis, design and testing of a novel direct-driven wave energy converter system. IET Renew Power Gener 2013;7(5):565–73.
[7] Elwood D, Yim SC, Prudell J, Stillinger C, von Jouanne A, Brekken T, et al. Design, construction, and ocean testing of a taut-moored dual-body wave energy converter with a linear generator power take-off. Renew Energy 2010;35(2):348–54.
[8] Wu F, Zhang XP, Ju P, Sterling MJH. Optimal control for an AWS-based wave energy conversion. IEEE Trans Power Syst 2009;24(4):1747–55.
[9] Mueller MA. Electrical generators for direct wave energy converters. IEE Proc. Generation, Transm Distribution 2002;149(4):446–56.
[10] Baker NJ. Linear generators for direct drive marine renewable energy converters. Doctoral thesis. School of Engineering University of Durham; 2003.
[11] Waters R, Stålberg M, Danielsson O, Svensson O, Gustafsson S, Strömstedt E, et al. Experimental results from sea trials of an offshore wave energy system. Appl Phys Lett 2007;90(3). 034105.
[12] Tyrberg S, Stålberg M, Boström C, Waters R, Svensson O, Strömstedt E, et al. The Lysekil wave power project: status update, WREC x Glasgow. July 2008.
[13] Lejerskog E, Gravråkmo H, Savin A, Strömstedt E, Haikonen K, Tyrberg S, et al. Lysekil research site, Sweden: a status update, proc. of the 9th European wave and tidal energy conference. September 2011. Southampton, UK.
[14] Eriksson M, Waters R, Svensson O, Isberg J, Leijon M. Wave power absorption: experiments in open sea and simulation. J Appl Phys 2007;102(8). 084910.
[15] Falnes J. A review of wave-energy extraction. Marine Structures 2007;20(4):185–201.
[16] Stålberg M, Waters R, Danielsson O, Leijon M. Influence of generator damping on peak power and variance of power for a direct drive wave energy converter. J Offshore Mech Arct Eng 2008;130(3).